ATTITUDE DETERMINATION AND CONTROL OF THE ASTEROIDFINDER MISSION

Ansgar Heidecker[1], **Markus Schlotterer**[2], **Stephan Theil**[3], **Marcus Hallmann**[4]

German Aerospace Center, Institut of Space Systems
Robert-Hooke-Straße 7, 28359 Bremen Germany

[1] *+49 421 24420-166, Ansgar.Heidecker@dlr.de*
[2] *+49 421 24420-118, Markus.Schlotterer@dlr.de*
[3] *+49 421 24420-113, Stephan.Theil@dlr.de*
[4] *+49 421 24420-110, Marcus.Hallman@dlr.de*

ABSTRACT

This paper presents concept and design of the attitude control system for the AsteroidFinder/SSB satellite. It describes the results that were obtained during Phase 0/A and extended Phase A of the project. The general system configuration is described and algorithms for attitude determination and control are presented. The base line design is an error state unscented KALMAN filter for the attitude determination and a linear quadric regulator approach for attitude control algorithm. Both algorithms have been integrated into a simulation environment for closed loop test and first results are presented.

1 INTRODUCTION

The German Aerospace Center (Deutsches Zentrum für Luft- und Raumfahrt e.V. - DLR) aims to build and operate a standard satellite bus (SSB) on its own. It will be suitable for multi-type missions and applications and shall enable independent and fast access to space for DLR's research institutes. It will also establish necessary capabilities and facilities for satellite development within DLR. DLR's Institute of Space Systems in Bremen (Germany) is supervising the program.

The SSB program is based on the Bi-Spectral-Infra-Red-Detection (BIRD) and the Technologie-Erprobungs-Träger (TET) satellite buses, which were built with contributions from DLR. It uses the experience and expertise gained during these two programs. BIRD was launched in October 2001 and is in its final operation phase today while TET is in development Phase C/D. The SSB is in Phase A/B and will extend the capabilities of these two programs to achieve a more sophisticated system which can be adapted to a broader range of mission requirements.

BIRD, TET and SSB are all compact satellites with an overall mass of approximately 100 kg to 150 kg. The dimensions of each satellite shall allow a piggy-back launch.

The primary payload of the first SSB is AsteroidFinder. AsteroidFinder is an optical telescope that will search for asteroids. The focus is placed on identifying and discovering asteroids with an orbit that is inside the Earth's orbit around the Sun. Such Asteroids and Inner Earth Objects (IEOs) could be a potential risk for the Earth. So far only a few IEOs have been discovered.

Due to the observation of astronomy targets the requirements that are placed on the Attitude Control System (ACS) are quite challenging. Especially with the restriction of the available hardware which is suitable for the compact satellite class.

The following paper presents the attitude control system design and presents the the preliminary algorithms.

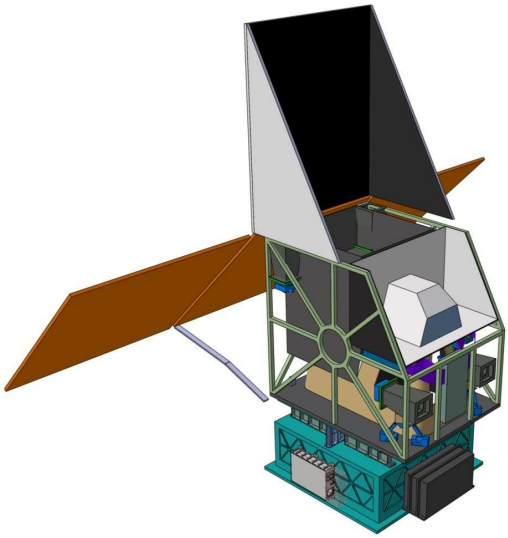

Fig. 1. Preliminary AsteroidFinder/SSB design [4]

2 MISSION CONCEPT

The AsteroidFinder/SSB (see Fig.1) will be used to identify inner earth orbit objects. To do this the region of observational interest for the AsteroidFinder/SSB mission is defined relative to the sun (at center). It ranges from -60° to -30° and +30° to +60° in ecliptic longitude relative to the sun and from -40° to +40° in ecliptic latitude relative to the sun.

To reach the scientific goal the AsteroidFinder telescope, which has a field of view of about 2°, has to be pointed towards a target area in inertial space. Each target area shall be observed for one minute. Afterwards the telescope shall be reoriented towards a new target and kept there again for one minute. The time to reorient and stabilize the telescope shall not exceed one minute. Besides this

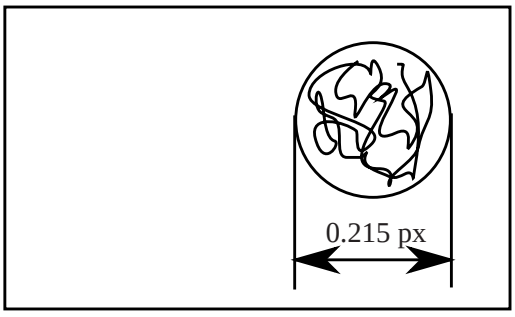

Fig. 2. Stability requirement for the CCD chip

first observation strategy another driving requirement is the pointing stability. The Charged Couple Device (CCD) of the telescope is sampling pictures at a frequency of 5 Hz. During on sample the modulus of the shift (see Fig. 2) of the imaged field on the focal plane shall be smaller than 0.215 px (3σ). Translated towards a preliminary stability value this means a pointing stability of < 7.5 arcsec/sec (3σ).

The pointing stability, the maneuverability and the ability to reuse BIRD and TET technologies lead towards a three axis stabilized spacecraft.

Fig. 3 shows a block diagram with the sensors and actuators that are used for the attitude control system and how they are connected with the spacecraft bus. The three axis stabilisation will use four reaction wheels arranged in a tetrahedron and three orthogonal arranged magnetic torquers. The

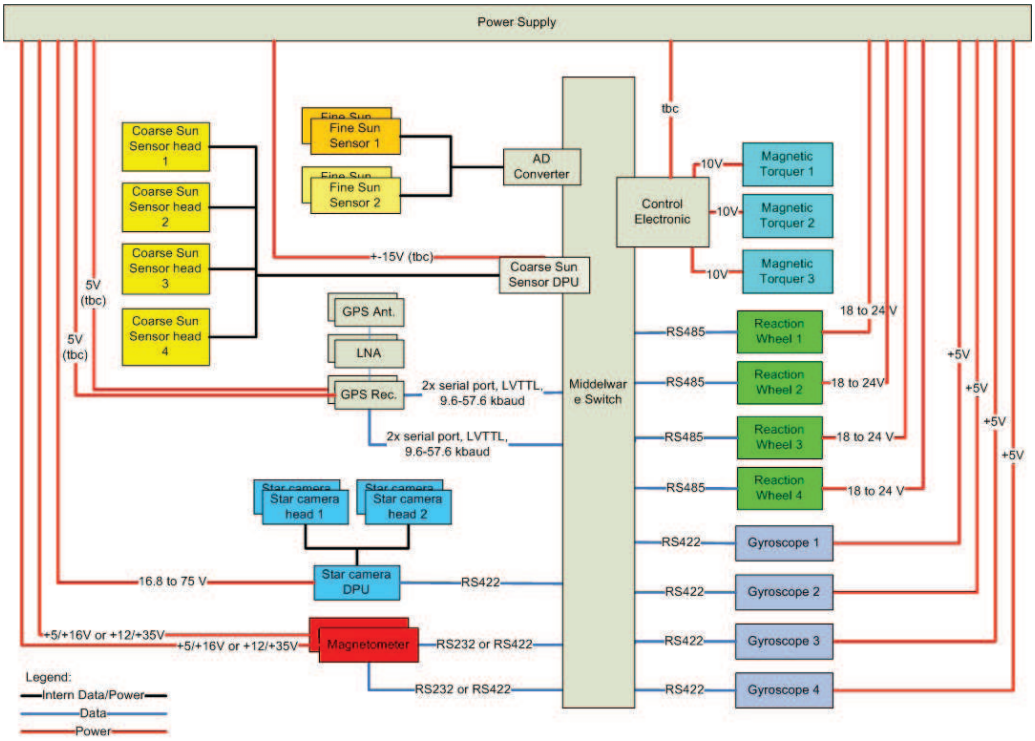

Fig. 3. Attitude control system block diagram

torques will be used for detumbling and desaturation of the reaction wheels while the wheels are used for fine pointing and maneuver control.

As high accuracy sensors a star camera and a set of four fiber optic gyros was chosen. In addition the telescope itself will be included in the control loop because it is the best available sensor. For coarse attitude maneuvers two different sun sensors and a magnetometer will be used.

During the ACS design the driving requirement was the pointing stability which should be reached. Therefore two things are important. The first one is a precise determination of the angular rates and the other one is a precise knowledge of disturbance torques that are introduced by the reaction wheel assembly.

3 ATTITUDE DETERMINATION

One issue is to identify and measure the attitude and especially the angular rates as good as possible. Therefore the idea is to use an unscented KALMAN filter (UKF) [7], [5], [6] for the high performance attitude determination algorithm. The UKF was developed during the 1990s by Simon J. Julier and Jeffrey K. Uhlmann and is based on the unscented transformation (UT). The UT allows to calculated the mean and covariance of a variable which is connected to another variable through a nonlinear function and omits a linearisation as it is used by an EKF. Thus it is possible to estimate the attitude dynamics in a more precise way.

3.1 Implementation of an UKF

The system state vector which is used for attitude determination will be a 10 dimensional vector. It consists of the attitude quaternion $\underline{q}$ and the angular rates of the satellite $\underline{\omega}_{sat}$. In addition a three dimensional disturbance torque vector $\underline{T}_D$ is added.

$$\underline{x} = [\underline{q}\ \underline{\omega}_{sat}\ \underline{T}_D]^T \tag{1}$$

The goal of the additional disturbance vector is to identify torques which can not be modeled directly. These are external disturbances which are introduced by the space environment and internal disturbances as they are produced by the reaction wheels.

Due to the properties of the UKF algorithm and quaternion algebra it is not advised to use quaternions directly [3] in the UKF algorithm. To solve this problem the UKF algorithm will use a nine dimensional error state vector $\Delta\underline{x}$ which is going to be estimated.

$$\Delta\underline{x} = [\Delta\underline{p}\ \Delta\underline{\omega}_{sat}\ \Delta\underline{T}_d] \tag{2}$$

Inside this vector $\Delta\underline{p}$ is the Generalized Rodrigues Parameter (GRP) representation of the error quaternion $\Delta\underline{q}$ which is defined as

$$\underline{q} = \Delta\underline{q} \otimes \hat{\underline{q}} \tag{3}$$

and where $\underline{q}$ is the true state. The conversion between a quaternion and a GRP is identified as

$$\underline{p} \equiv f\frac{q_{123}}{a+q_4} \tag{4}$$

While the inverse transformation to recover the quaternion from equation 4 is given by

$$q_4 = \frac{-a\left\|\underline{p}\right\|^2 + f\sqrt{f^2+(1-a^2)\left\|\underline{p}\right\|^2}}{f^2+\left\|\underline{p}\right\|^2} \tag{5}$$

$$q_{123} = f^{-1}(a+q_4)\underline{p} \tag{6}$$

In this definition f is a scale factor and a a parameter from 0 to 1. For first evaluation purposes the choice of these parameters follows the advice of [3] such that $f = 2(a+1)$ and $\underline{p}$ is equal to the rotation angle θ for small errors. The usage of the GRPs transforms the error quaternion into an unconstrained representation which is suitable for the UKF algorithm.

The remaining error angular rate and disturbance torque are described as:

$$\underline{\omega}_{sat} = \hat{\underline{\omega}}_{sat} + \Delta\underline{\omega}_{sat} \tag{7}$$

$$\underline{T}_d = \hat{\underline{T}}_d + \Delta\underline{T}_d \tag{8}$$

With such a description only the evolution of the errors has to be described inside the UKF while for the propagation of the full state vector the full system dynamics (Eq. 9 - 10) can be used [14], [11].

$$\dot{\underline{q}}(t) = \frac{1}{2}\,\underline{\underline{\Omega}}(\underline{\omega}_{sat}(t))\,\underline{q}(t) \tag{9}$$

$$\dot{\underline{\omega}}_{sat}(t) = \underline{\underline{I}}_{sat}^{-1}\left(\underline{T}_D(t) - \underline{\omega}_{sat}(t)\times\underline{L}_{sat}(t) - \underline{\omega}_{sat}(t)\times\underline{L}_{rw}(t) - \dot{\underline{L}}_{rw}(t)\right) \tag{10}$$

In difference to an EKF the UKF does not require any linearisation and can use the nonlinear error dynamics $f(\Delta\underline{x}) = \Delta\underline{\dot{x}}$ directly. Therefore three differential equations are used inside the UKF.

$$\Delta\underline{\dot{p}} = -\underline{\omega} \times \Delta\underline{p} + \Delta\underline{\omega} - \frac{1}{2}\Delta\underline{\omega} \times \Delta\underline{p} \tag{11}$$

$$\Delta\underline{\dot{\omega}} = \underline{\underline{I}}^{-1}\left[\Delta\underline{T}_d - \underline{\omega} \times \underline{\underline{I}}\,\Delta\underline{\omega} - \Delta\underline{\omega} \times \underline{\underline{I}}\underline{\omega} - \Delta\underline{\omega} \times \underline{\underline{I}}\Delta\underline{\omega} - \Delta\underline{\omega} \times \underline{L}_{rw}\right] \tag{12}$$

$$\Delta\underline{\dot{T}}_d = 0 \tag{13}$$

Equation 11 is an approximation of the true attitude error [3] but for a first evaluation this is a sufficient starting point. For the evolution of the angular rate error the full error dynamics [12], [1] are used while the disturbance torques are assumed to be constant over one integration step.

For the internal propagation scheme these error dynamics are used and they are solved by numerical integration. At the end of one estimation step the errors are combined with the full propagated state vector which is done by equation 9 and 10. The GRP is converted towards a quaternion and multiplied with the propagated quaternion while the angular rate and the disturbance torque can be simply summed up with the full state. For the new estimation the error state is reset to zero while the error state covariance matrix is re-used for the next UKF loop.

For evaluation purposes the measurement equation were kept as simple as possible. Therefore the quaternion and the angular rate are assumed to be measured directly. These measurements are compared with the propagated full state before their differences are forwarded to the UKF algorithms. This allows to represent the measured as well as the propagated quaternion as a GRP. Furthermore the measurement equation 14 became quite simple.

$$h(\Delta\underline{x}) = \begin{bmatrix} \Delta\underline{p} \\ \Delta\underline{\omega}_{sat} \\ \Delta\underline{\omega}_{sat} \end{bmatrix} \tag{14}$$

The double usage of the angular rate is used to represent the fiber optic gyro measurements and the telescope measurements. The whole UKF system was implemented as a Matlab/Simulink block diagram to evaluate the estimation algorithm.

3.2 Preliminary Results

For the first test the satellite system was modeled with a diagonal moment of inertia tensor with 4 kgm^2 and an overall mass of about 100 kg. The measurements uncertainties were modeled as the original state vector values corrupted with white noise. Additional a disturbance torque was entering the dynamic system. The magnitude of the errors where chosen to reflect common sensors. In detail these values where:

- Star camera - quaternion measurement with 1 Hz update rate and a standard deviation of $3\sigma = 45 \cdot 10^{-6} \approx 9$ arcsec
- Telescope - angular rate measurement with 5 Hz update rate and a standard deviation of $3\sigma = 14.4 \cdot 10^{-6}$ rad/s ≈ 3 arcsec/s
- Fiber optic gyroscope assembly - angular rate measurement with 10 Hz update rate and a standard deviation of $3\sigma = 4.2 \cdot 10^{-5}$ rad/s ≈ 8.6 arcsec/s

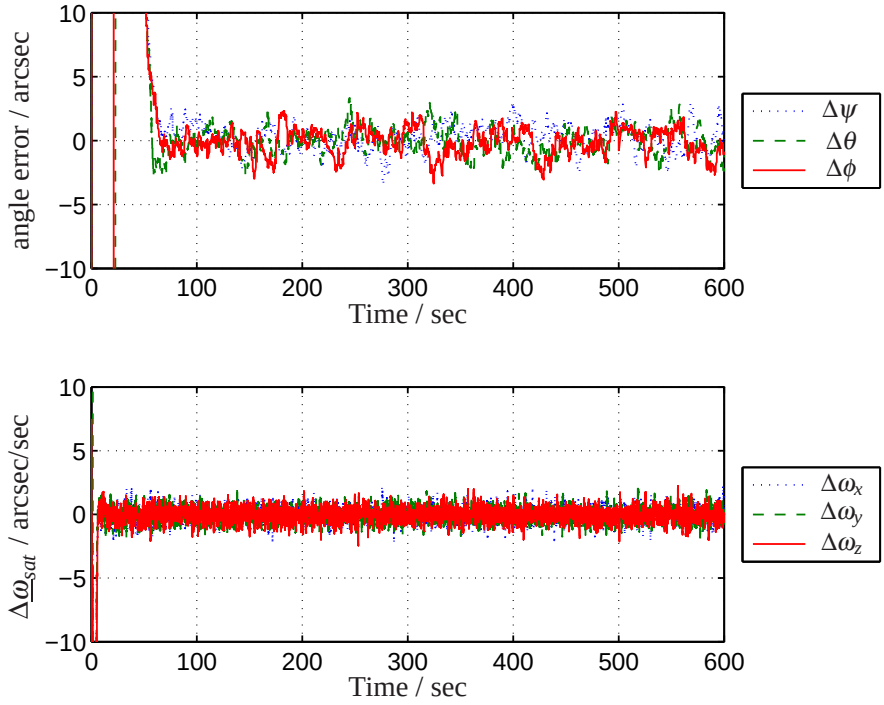

Fig. 4. Estimation error of the tuned unscented KALMAN filter towards the true state

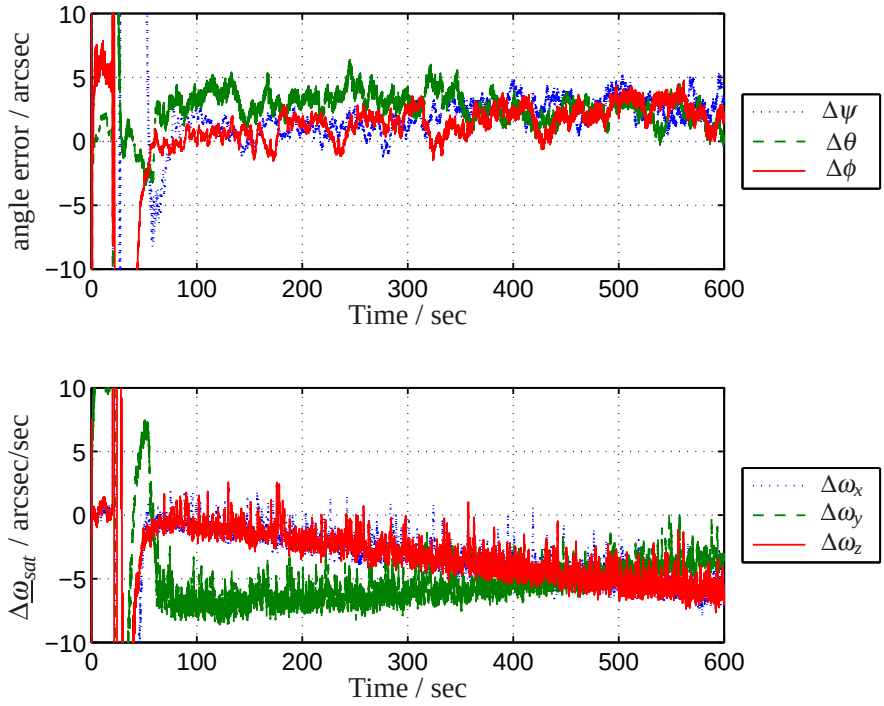

Fig. 5. Estimation error of the tuned extended KALMAN filter towards the true state. Configured with the same covariance matrices as the UKF

- Disturbance Torque - slowly varying sine wave with an amplitude of $2 \cdot 10^{-4}$ Nm, a frequency of $1.7 \cdot 10^{-3}$ rad/sec and an additional white noise with the standard deviation of $3\sigma = 0.21 \cdot 10^{-3}$ Nm. The magnitude of the sine wave was chosen to reflect the magnitude of the external disturbances.

Furthermore the system dynamic covariance $\underline{\underline{Q}}$ and the measurement covariance $\underline{\underline{R}}$, which are used in every KALMAN filter, were chosen as diagonal matrices to reflect the model and measurement uncertainties. Both matrices where chosen as a diagonal matrix with their main diagonal holding the information of the variance.

$$\underline{\underline{Q}} = \begin{pmatrix} I_{[3\times3]} \cdot \sigma_p^2 & 0_{[3\times3]} & 0_{[3\times3]} \\ 0_{[3\times3]} & I_{[3\times3]} \cdot \sigma_\omega^2 & 0_{[3\times3]} \\ 0_{[3\times3]} & 0_{[3\times3]} & I_{[3\times3]} \cdot \sigma_{T_D}^2 \end{pmatrix} \tag{15}$$

$$\underline{\underline{R}} = \begin{pmatrix} I_{[3\times3]} \cdot \sigma_{ST}^2 \\ I_{[3\times3]} \cdot \sigma_{P/L}^2 \\ I_{[3\times3]} \cdot \sigma_{FOG}^2 \end{pmatrix} \tag{16}$$

In a suitable configuration the values for the standard deviation where tuned to

$$\begin{aligned} \sigma_p &= 1.225 \cdot 10^{-4} \\ \sigma_\omega &= 0.0175 \cdot 10^{-4} \\ \sigma_{T_D} &= 0.07 \cdot 10^{-4} \\ \sigma_{ST} &= 15 \cdot 10^{-6} \\ \sigma_{P/L} &= 4.8 \cdot 10^{-6} \\ \sigma_{FOG} &= 1.4 \cdot 10^{-5} \end{aligned}$$

The measurement covariance uses exactly the same values as they where chosen for the sensors while the standard deviation of the disturbance torque was chosen ten times smaller than the expected disturbance torques. The deviation of the angular rate was chosen as σ_{T_D} divided by four which shall reflect the coupling through the moment of inertia. The deviation of the GRP was tuned through several simulation runs.

In addition to the covariance matrices the UKF requires the choice of the three remaining scaling parameters.

$$\begin{aligned} \alpha &= 1 \cdot 10^{-3} \\ \beta &= 2 \\ \kappa &= 0 \end{aligned}$$

Their choice follows a suggestion of [10] which results in a sufficient sigma point set.

Fig. 4 shows the results of the tuned version of the UKF which was tested in the control loop. The x-axis is indicating the time in seconds. The upper diagram is the angle deviation and the lower diagram the angular rate deviation. Under perfect conditions both diagrams would show a straight line at y = 0. After an initial settling phase it can be seen that the UKF is able to determine the actual attitude up to an error of 2.5 arcsecond and the angular rate error up to 1 arcsec/sec.

For comparison Fig. 5 shows the results for the same state vector implemented in an extended KALMAN filter. Here the same configuration was used as it was used for the UKF. It can be seen clearly that the UKF is able to supersede the EKF. The main disadvantage of the EKF is that it is not able to cover the disturbance torques correctly and therefore the angular rate estimation is drifting. In contrast to this the UKF is able to cover these disturbance torques and can give a better estimation as the EKF. Due to this reason the UKF will be studied in more detailed in the upcoming Phases.

4 ATTITUDE CONTROL

The second essential task for the AsteroidFinder/SSB is attitude control. During Phase 0/A two basic controllers were investigated for inertial pointing. The first one was a simple proportional derivative (PD) controller while the second one is a proportional integral derivative (PID) controller. Both controllers are using a static gain which is found by a linear quadric Gaussian (LQG) control scheme. The following section will focus on the PID controller, due to the fact that this one is more accurate than the simple PD controller.

4.1 Restriction to Linear System Dynamic

Due to the choice of a linear control design there are two restrictions which have to be taken into account for the further design. These two restrictions are the choice of an operating point and the assumption of uncoupled dynamics of all three axis at that point.

The linearisation itself will be performed at the operating point $\underline{q}_0 = (0\ 0\ 0\ 1), \underline{\omega}_0 = (0\ 0\ 0)$. To ensure that this mathematical description is valid for all desired states the control should work all the time around this operating point. To achieve this only the errors of the state will be given to the control law which is equal to an operation around the zero point.

$$\Delta\underline{q} = \underline{q}_D \otimes \hat{\underline{q}}^{-1} \tag{17}$$

$$\Delta\underline{\omega}_{sat} = \underline{\omega}_D - \hat{\underline{\omega}}_{sat} \tag{18}$$

Here $_D$ identifies the desired values while $\hat{}$ are the measured values that were processed by the attitude determination. If the guidance is changing the desired $_D$ values the error is increasing and therefor the attitude control is activated. The formulation of this error allows the controller to work all the time around the zeroth point.

Another effect of linearisation is the omission of two terms of the systems dynamics equations $\dot{\underline{\omega}}_{sat}$ 10. These terms (see Eqs. 19-20) are describing the coupling torque between the three axis of the satellite and the coupling between the satellite and the reaction wheels.

$$\underline{T}_{C,sat} = \underline{\omega}_{sat} \times \underline{L}_{sat} \tag{19}$$

$$\underline{T}_{C,sat,rw} = \underline{\omega}_{sat} \times \underline{L}_{rw} \tag{20}$$

The problem is that these two terms will act as an unknown disturbance torque although they are well known. Too get a more precise control algorithm it is important to address theses two terms. One way to do this is to use a feedforward control [9], [13] which is able to cancel known disturbances. During the controller design it was realized that without feedforward control the induced disturbances are to big to ensure a precise attitude control system.

4.2 Linear System Dynamic

On the satellite system the system itself has to have a linearised form. The linearised model shall fit into the standard form of a linear state space system which can be found in many textbooks [2],[13], [8], [9].

$$\dot{\underline{x}}(t) = \underline{\underline{A}}(t)\,\underline{x}(t) + \underline{\underline{B}}(t)\,\underline{u}(t) + \underline{\underline{E}}(t)\,\underline{z}(t) \tag{21}$$

$$\underline{y}(t) = \underline{\underline{C}}(t)\,\underline{x}(t) + \underline{\underline{D}}(t)\,\underline{u}(t) \tag{22}$$

Where $\underline{x}(t)$ is the state of the system, $\underline{u}(t)$ is the control signal, $\underline{z}(t)$ are the disturbances and $\underline{y}(t)$ is the output of the system. The matrix $\underline{\underline{A}}(t)$ is the state matrix, $\underline{\underline{B}}(t)$ is the input matrix, $\underline{\underline{C}}(t)$ the output matrix, $\underline{\underline{D}}(t)$ the input to output coupling matrix and $\underline{\underline{E}}(t)$ the disturbance matrix.

To be able to use a linear control strategy this system dynamics have to be linearised around an operating point $()_0$. The choice of the operating point was done in such a way that the dynamics became quite simple. With the help of the two restrictions of the operating point and a decoupled behavior of all satellite axis the linearised system matrices can be determined.

$$\underline{\underline{A}} = \left[\begin{array}{cc} \frac{\partial \dot{\underline{q}}}{\partial \underline{q}} & \frac{\partial \dot{\underline{q}}}{\partial \underline{\omega}_{sat}} \\ \frac{\partial \dot{\underline{\omega}}_{sat}}{\partial \underline{q}} & \frac{\partial \dot{\underline{\omega}}_{sat}}{\partial \underline{\omega}_{sat}} \end{array}\right]_{\underline{q}_0, \underline{\omega}_{sat,0}} \tag{23}$$

$$\underline{\underline{B}} = \left[\begin{array}{c} \frac{\partial \dot{\underline{q}}}{\partial \underline{T}_c} \\ \frac{\partial \dot{\underline{\omega}}_{sat}}{\partial \underline{T}_c} \end{array}\right]_{\underline{q}_0, \underline{\omega}_{sat,0}} \tag{24}$$

$$\underline{\underline{C}} = \left[\begin{array}{ccc} 1 & 0 & \dots \\ 0 & 1 & \\ \vdots & & \ddots \end{array}\right] \tag{25}$$

$$\underline{\underline{D}} = \underline{\underline{0}} \tag{26}$$

Where $\underline{T}_c = \dot{\underline{L}}_{rw}$ is the control torque. The calculation of the JACOBIAN matrices can be done in straight forward manner. In addition the state vector can be reduced by one value due to the choice of $q_{0,4} = 1$. With the characteristics of the new operating point the linearized dynamics can be defined.

$$\underline{\underline{A}} = \left[\begin{array}{cc} 0_{[3\times3]} & I_{[3\times3]} \cdot 0.5 \\ 0_{[3\times3]} & 0_{[3\times3]} \end{array}\right] \tag{27}$$

$$\underline{\underline{B}} = \left[\begin{array}{c} 0_{[3\times3]} \\ \underline{\underline{I}}_{sat}^{-1} \end{array}\right] \tag{28}$$

These are the dynamics of a continuous linearised system that represents the nonlinear continuous satellite dynamics. The design of a control gain can be done with the help of this continues linear system.

4.3 Linear Quadric Gaussian Control

The basic idea behind the Linear Quadric Gaussian Control (LQG) is to transfer a system optimal from an initial state $\underline{x}_0$ to the final state $\underline{x}_f = \underline{0}$. To do this LQG calculates a control gain $\underline{\underline{K}}(t)$ and multiply this with the state to derive a control command $\underline{u}(t)$.

$$\underline{u}(t) = -\underline{\underline{K}}(t)\,\underline{x}(t) \tag{29}$$

To find the control gain LQG is minimizing a quadric cost function J, which relates the system state $\underline{x}$ and the control input $\underline{u}$ to each other [2], [8].

$$J(\underline{x}(t), \underline{u}(t)) = \frac{1}{2}\int_0^\infty \underline{x}^T(t)\,\underline{\underline{Q}}\,\underline{x}(t) + \underline{u}^T(t)\,\underline{\underline{R}}\,\underline{u}(t)dt \tag{30}$$

The matrices $\underline{\underline{Q}}$ and $\underline{\underline{R}}$ are positive, symmetric and definite weighting matrices that define the term "optimal". They have to be specified for each problem. The matrix $\underline{\underline{K}}(t)$ which minimize this cost function is the optimal control gain for the system.

If the optimization horizon is set to infinity ($t = \infty$) the control gain reaches a steady state. Due to that fact the calculation of the optimal control gain simplifies to the solution of

$$\underline{\underline{K}} = \underline{\underline{R}}^{-1}\,\underline{\underline{B}}^T\,\underline{\underline{P}}(t) \tag{31}$$

where $\underline{\underline{P}}$ is the solution of the following matrix RICCATI equation.

$$\dot{\underline{\underline{P}}}(t) = \underline{\underline{A}}^T\,\underline{\underline{P}}(t) + \underline{\underline{P}}(t)\,\underline{\underline{A}} - \underline{\underline{P}}(t)\,\underline{\underline{B}}\,\underline{\underline{R}}^{-1}\,\underline{\underline{B}}^T\,\underline{\underline{P}}(t) + \underline{\underline{Q}} \tag{32}$$

$$\dot{\underline{\underline{P}}}(t_\infty) = \underline{\underline{0}} \tag{33}$$

This equation can be solved by numerical integration [8], [2] and allows the computation of the optimal control gain. Another advantage of the LQG method is that it generates a stable control gain for a linear system.

4.4 Controller Design

During the controller development it was seen that a simple PD-controller is not able to perform the required tasks. The solution to this problem is an integrating gain which leads to a proportional integral derivative controller (PID).

To be able to use the LQG approach the system dynamics have to be extended by an integrating state $\underline{e}$. This state should include the integral of the error quaternion. The system state is therefore defined as

$$\underline{x} = \begin{pmatrix} \Delta\delta\underline{q} \\ \Delta\underline{\omega} \\ \underline{e} \end{pmatrix} \tag{34}$$

With this new state the linearised system dynamics have to be extended in the following way.

$$\underline{\underline{A}} = \begin{bmatrix} 0_{[3\times3]} & I_{[3\times3]} \cdot 0.5 & 0_{[3\times3]} \\ 0_{[3\times3]} & 0_{[3\times3]} & 0_{[3\times3]} \\ I_{[3\times3]} \cdot 1 & 0_{[3\times3]} & 0_{[3\times3]} \end{bmatrix} \tag{35}$$

$$\underline{\underline{B}} = \begin{bmatrix} 0_{[3\times3]} \\ \underline{\underline{I}}_{sat}^{-1} \\ 0_{[3\times3]} \end{bmatrix} \tag{36}$$

It should be mentioned that for the control gain design only the first equation of the linear system dynamics (equation 21) has to be adapted. The upper left part of $\underline{\underline{A}}$ and the upper part of $\underline{\underline{B}}$ still stay the same as they are defined in the linearised system dynamics but they are extended about the integral part for $\Delta\delta\underline{q}$

The next step is the choice of two sufficient weighting matrices. For the PID-controller they are defined in the following way.

$$\underline{\underline{Q}} = \begin{bmatrix} I_{[3\times3]} \cdot \sigma_{\delta q} & 0 & 0 \\ 0 & I_{[3\times3]} \cdot \sigma_{\omega} & 0 \\ 0 & 0 & I_{[3\times3]} \cdot \sigma_{e} \end{bmatrix} \tag{37}$$

$$\underline{\underline{R}} = I_{[3\times3]} \cdot \sigma_{T_c} \tag{38}$$

The single σ values are defined as.

$$\sigma_{\delta q} = 1 \tag{39}$$

$$\sigma_{\omega} = 1000 \tag{40}$$

$$\sigma_{e} = 10 \tag{41}$$

$$\sigma_{T_c} = 10 \tag{42}$$

The choice of these values is addressing the fact that the angular rate error has highest priority. The angle itself is treated as less important and while the error integral of the error and the controller input are weighted in the same way. These values are only reflecting the first analysis which as done during Phase 0/A and shall represent the order of magnitude. In the next Phases these values have to be adjusted and further defined.

The control gains that were designed for this case are

$$\underline{\underline{K}}_{PID,c} = \begin{pmatrix} 6.7198 & 0 & 0 & 11.2641 & 0 & 0 & 1 & 0 & 0 \\ 0 & 6.7198 & 0 & 0 & 11.2641 & 0 & 0 & 1 & 0 \\ 0 & 0 & 6.7198 & 0 & 0 & 11.2641 & 0 & 0 & 1 \end{pmatrix} \tag{43}$$

$$\underline{\underline{K}}_{PID,5Hz} = \begin{pmatrix} 5.2467 & 0 & 0 & 8.9330 & 0 & 0 & 0.7687 & 0 & 0 \\ 0 & 5.2467 & 0 & 0 & 8.9330 & 0 & 0 & 0.7687 & 0 \\ 0 & 0 & 5.2467 & 0 & 0 & 8.9330 & 0 & 0 & 0.7687 \end{pmatrix} \tag{44}$$

where the discrete gain is for a sampling time of $\Delta t = 0.2$ s.

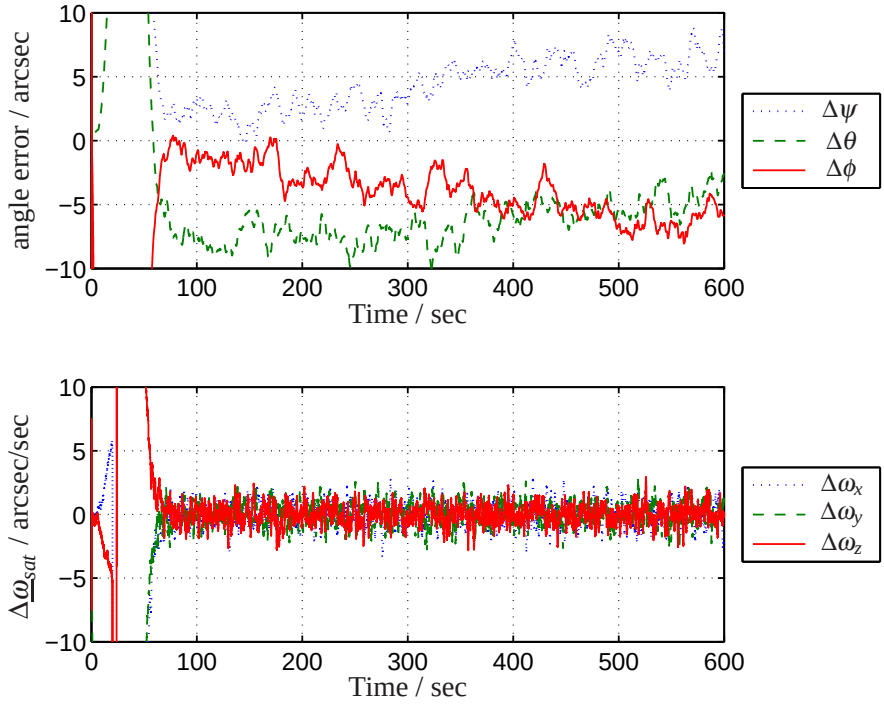

Fig. 6. Pointing error of the closed loop system with a 5 Hz PID-controller and an UKF attitude determination during inertial pointing.

For preliminary testing the attitude controller was tested during inertial pointing. In this operation phase the desired attitude is fixed in inertial space and the angular rates are zero. Fig. 6 shows the errors of the attitude controller. During this test the simulation was started and the attitude controller was activated at t = 20 s. The requirement for the angular rates was to stay below the values of 7.5 arcsec/sec which could be achieved after a transient phase. In contrast to this the angle deviation is larger than the angular rate deviation which is a result of the chosen weighting matrices for the controller.

5 CONCLUSION

With the work of the Phase 0/A a preliminary design of the AsteroidFinder/SSB attitude control system was established. This design in able to fulfill the requirements. Two primary algorithms for attitude determination and control where presented. It could be seen that the unscented KALMAN filter gives sufficient results which has to be investigated in more detailed in the upcoming Phase B. Especially the computational load compared to an extended KALMAN filter has to be checked and a detailed filter tuning has to be performed.

The attitude control algorithm design will keep on following a linear quadric Gaussian approach due to the fact that it is simple to handle and had shown its capabilities. Additionally a full guidance

profile has to be defined and combined with the attitude controller for the slew mode. Further the disturbances which are going to be introduce in the different parts of the system have to be studied in more detail.

Nevertheless the it can be said that the preliminary design of the AsteroidFinder/SSB attitude control system is able to fulfill the requirements and will be further developed.

REFERENCES

[1] T. Bak. *Spacecraft Attitude Determination, a Magnetometer Approach*. PhD thesis, Aalborg University, Department of Control Engineering, 1999.

[2] J. Burl. *Linear optimal control: H 2 and H ∞ methods*. Addison-Wesley, Menlo Park, Calif., 1999.

[3] J. Crassidis and F. Markley. Unscented Filtering for Spacecraft Attitude Estimation. *Journal of Guidance, Control, and Dynamics*, 26(4):536–542, 2003.

[4] J. Hartmann and M. Lieder. *Kompaktsatellit AsteroidFinder/SSB Delta Phase A: Structure and Accomodation*. Institut für Raumfahrtsysteme (Bremen), March 3rd, 2009.

[5] S. Julier. The Scaled Unscented Transformation. In *Proceedings of the 2002 American Control Conference, ACC: May 8 - 10, 2002, Hilton Anchorage and Egan Convention Center, Anchorage, Alaska, USA*, pages 4555–4559. IEEE Service Center, 2002.

[6] S. Julier and J. Uhlmann. Unscented filtering and nonlinear estimation. *PROCEEDINGS OF THE IEEE*, 2004.

[7] S. Julier, J. Uhlmann, and H. Durrant-Whyte. A New Approach for Filtering Nonlinear Systems. *Proceedings of the American Control Conference*, pages 1628–1623, 1995.

[8] J. Lunze. *Mehrgrößensysteme, digitale Regelung: Mit 53 Beispielen, 91 Übungsaufgaben sowie einer Einführung in das Programmsystem MATLAB*, volume 2 of *Springer-Lehrbuch*. Springer, Berlin, 4., neu bearb. aufl. edition, 2006.

[9] H. Lutz and W. Wendt. *Taschenbuch der Regelungstechnik: Mit MATLAB und Simulink*. Deutsch, Frankfurt am Main, 7., erg. aufl. edition, 2007.

[10] G. Mohinder and A. Angus. *Kalman filtering: Theory and practice using MATLAB*. Wiley, Hoboken, NJ, 3. ed. edition, 2008.

[11] J. M. Sidi. *Spacecraft dynamics and control: A practical engineering approach*, volume 7 of *Cambridge aerospace series*. Cambridge Univ. Press, Cambridge, 1997.

[12] S. Theil and M. Wiegand. High Accuracy Attitude Determination and Control of the DIVA Mission. In R. Bishop, editor, *Spaceflight mechanics 1999: Proceedings of the AAS/AIAA Space Flight Mechanics Meeting held February 7 - 10, 1999, Breckenridge, Colorado*, volume 102 of *Advances in the astronautical sciences*, pages 943–960. Univelt, 1999.

[13] P. Vörsmann. *Regelungstechnik 1: Umdruck zur Vorlesung*. Institut für Luft- und Raumfahrtsysteme, Braunschweig, WS 2004/05.

[14] J. R. Wertz. *Spacecraft attitude determination and control*, volume 73 of *Astrophysics an*. Kluver Acad. Publ, Dordrecht, reprint edition, 2002.

◄ BACK TO SESSION DETAILED CONTENTS ◄ BACK TO HIGHER LEVEL CONTENTS